JACS
JOURNAL OF THE AMERICAN CHEMICAL SOCIETY
pubs.acs.org/JACS
Article

Catalytic Structure Design by AI Generating with Spectroscopic Descriptors

Tongtong Yang,[#] Donglai Zhou,[#] Sheng Ye,[#] Xiyu Li,[#] Huirong Li, Yi Feng, Zifan Jiang, Li Yang, Ke Ye, Yixi Shen, Shuang Jiang, Shuo Feng, Guozhen Zhang, Yan Huang,* Song Wang,* and Jun Jiang*

Cite This: J. Am. Chem. Soc. 2023, 145, 26817−26823
Read Online
ACCESS | Metrics & More | Article Recommendations | Supporting Information

ABSTRACT: Generative artificial intelligence has depicted a beautiful blueprint for on-demand design in chemical research. However, the few successful chemical generations have only been able to implement a few special property values because most chemical descriptors are mathematically discrete or discontinuously adjustable. Herein, we use spectroscopic descriptors with machine learning to establish a quantitative spectral structure−property relationship for adsorbed molecules on metal monatomic catalysts. Besides catalytic properties such as adsorption energy and charge transfer, the complete spatial relative coordinates of the adsorbed molecule were successfully inverted. The spectroscopic descriptors and prediction models are generalized, allowing them to be transferred to several different systems. Due to the continuous tunability of the spectroscopic descriptors, the design of catalytic structures with continuous adsorption states generated by AI in the catalytic process has been achieved. This work paves the way for using spectroscopy to enable real-time monitoring of the catalytic process and continuous customization of catalytic performance, which will lead to profound changes in catalytic research.

INTRODUCTION

Catalysts have attracted a great deal of attention from researchers because they can enhance the efficiency and selectivity of chemical reactions, reduce the consumption of energy and resources, and mitigate the environmental impact of industrial processes.[1,2] Modulating catalytic performance by regulating the relative position between adsorbed molecules and catalysts is a promising vision for achieving catalytic customization.[3,4] However, it is extremely difficult to characterize the molecular positions accurately by the experiment.[5] Moreover, there is a large amount of redundancy in the search space based on structural features as many structures are chemically implausible.[6] Even worse, due to the lack of a suitable experimental indicator to determine the catalytic states in real time,[7,8] one has to adjust the catalytic states first and then perform the performance test, which creates a timing disconnect problem. Even if the desired catalytic state is found by a time-consuming trial-and-error approach, it is accidental and discontinuous. Thus, even for single-atom catalysts with relatively simple structures,[9−11] generating continuous catalytic states such as molecular adsorption energy is also still a formidable challenge.

In recent years, the rapid development of in situ ultrafast spectroscopy has made it possible to monitor the catalytic state. Several studies have shed light on the underlying mechanisms of catalytic processes through in situ surface-enhanced or operando spectroscopy,[12−14] which can identify the intermediates and active sites, as well as uncover the dynamics of structure during the catalytic process. However, in experiments, the interpretation of spectra still heavily relies on the experience of well-trained experts, which are qualitative and nonimmediate.[15,16] Meanwhile, first-principles calculations are also commonly used to interpret the spectra, but such a theoretical trial-and-error approach is also inefficient and cannot meet the interpretation requirements for large amounts of experimentally generated spectral data.[17,18] This all limits the applicability and scalability of spectroscopic techniques for catalytic research and development. For mining the implied spectral information, machine learning (ML) has given a glimpse of achieving breakthroughs.[19−21] ML can be used to exact useful features from spectra, to establish correlations between spectra and catalyst properties or structures and to optimize catalyst design based on spectral feedback. As a

Received: August 25, 2023
Revised: November 17, 2023
Accepted: November 20, 2023
Published: November 29, 2023

https://doi.org/10.1021/jacs.3c09299
J. Am. Chem. Soc. 2023, 145, 26817−26823

physically meaningful quantity, the spectra have been used directly as descriptors for predicting catalytic properties.[22,23] However, the implementation of dynamic structural inversion and continuous catalytic generation based on spectroscopic descriptors is still to be developed.

In this work, we established a quantitative spectra structure−property relationship through ML of vibrational spectroscopy and achieved both structure inversion and catalytic generation based on the spectroscopic descriptors. Single-atom catalysts (SACs) with metal atoms dispersed on metal oxide carriers[24,25] were used as an example to investigate the quantitative relationship between the adsorption states (properties and structures) and the spectral characteristics of key intermediate molecules CO during the carbon dioxide reduction reaction (CO_2RR).[26,27] We developed an ML model (ML-1) for investigating properties, including adsorption energy (E_{ads}) and charge transfer (Δq), and another ML model (ML-2) for inversing structures of the adsorbed molecule CO. Six structural parameters including bond lengths, bond angles, and dihedral angle were predicted by using the IR spectral signals of CO (Figure S1). By utilizing these parameters, we can precisely determine the location of small molecules relative to the monatomic catalyst. Then, the spatial relative coordinates of the CO molecule can be uniquely determined, which achieves structure inversion. This is a novel method to obtain structural information from spectra without relying on theoretical calculations or experimental assumptions. Furthermore, an AI-generating workflow for catalytic structure design based on the above two ML models was then developed (Figure 1). First, a large number of spectra are randomly generated for rapid prediction of adsorption energy. By comparing them with the desired adsorption energy, the spectral generation process is iterated to find the spectrum corresponding to the desired properties. Then, the structure of the CO molecule is inverted based on this spectrum, and its property is verified via density functional theory calculations.

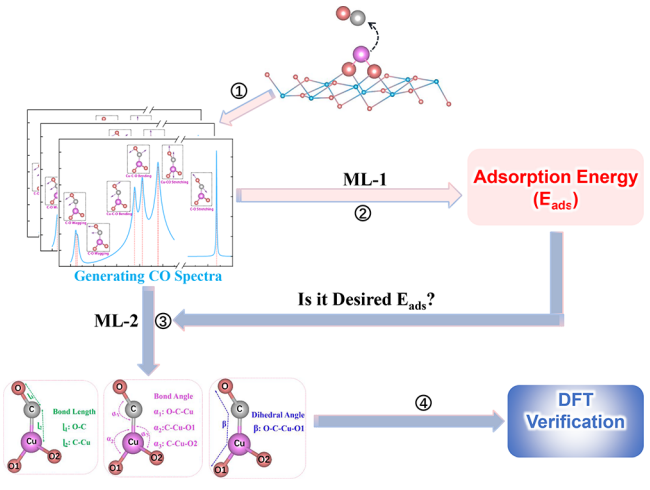

Figure 1. Flowchart of designing a catalytic structure with desired adsorption energy by spectroscopic descriptors. (1) Calculated the spectra of CO adsorbed on a monometallic supported metal oxide catalyst and then randomly generated a large number of CO spectra. (2) CO spectra predicted adsorption energy by ML-1 model. (3) Screened the CO spectra based on desired adsorption energy and then predicted CO structure information by ML-2 model. (4) Verification of adsorption energy using the density functional theory (DFT) method.

So far, we have been able to use spectroscopy as an indicator to continuously design the catalytic structures with desired properties. This work not only quantified the spectra structure−property relationship but also paved the way for catalytic customization through in situ ultrafast spectroscopy.

RESULTS AND DISCUSSION

First of all, we selected Cu-SAC loaded on TiO_2 as the substrate to investigate its adsorption behaviors with the CO molecule (Figure 2a). To capture as many adsorption states as

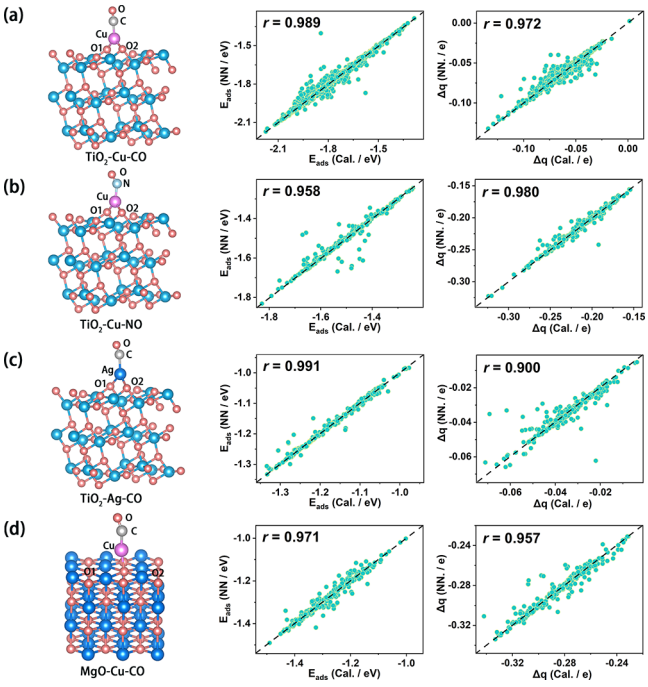

Figure 2. Predicted results of the ML-1 model for catalytic properties including adsorbed molecular adsorption energy and charge transfer. (a) System of TiO_2−Cu−CO. (b−d) Transfer systems of TiO_2−Cu−NO, TiO_2−Ag−CO, and MgO−Cu−CO, respectively.

possible, molecular dynamics (MD) simulations were performed at different temperatures, and about 12,000 adsorption configurations were extracted from the trajectories of MD simulations. Next, a cluster unit was cut from each periodic structure for IR spectral calculations at the first-principles level. We acknowledged that the theoretical spectrum might not perfectly match the real spectrum due to its Lorentzian shape. Nonetheless, various methods and techniques made it possible to establish successful correlations between the theoretical and experimental spectra.[28,29] The primary aim of these methods was to extract relevant data from the spectrum, specifically the positions, shifts, and shapes of peaks, which ultimately affected the catalytic activity. Thus, we believe that the theoretical spectra can capture the essential characteristics of the adsorption process. The catalytic properties, including adsorption energy and charge transfer, were also investigated with first-principles calculations. Meanwhile, for each adsorption configuration, two bond lengths, three bond angles, and one dihedral angle were collected through an in-house developed automatic script (Figure 1). Then, the neural networks were constructed for predicting the above catalytic properties and spatial relative coordinates from

https://doi.org/10.1021/jacs.3c09299
J. Am. Chem. Soc. 2023, 145, 26817−26823

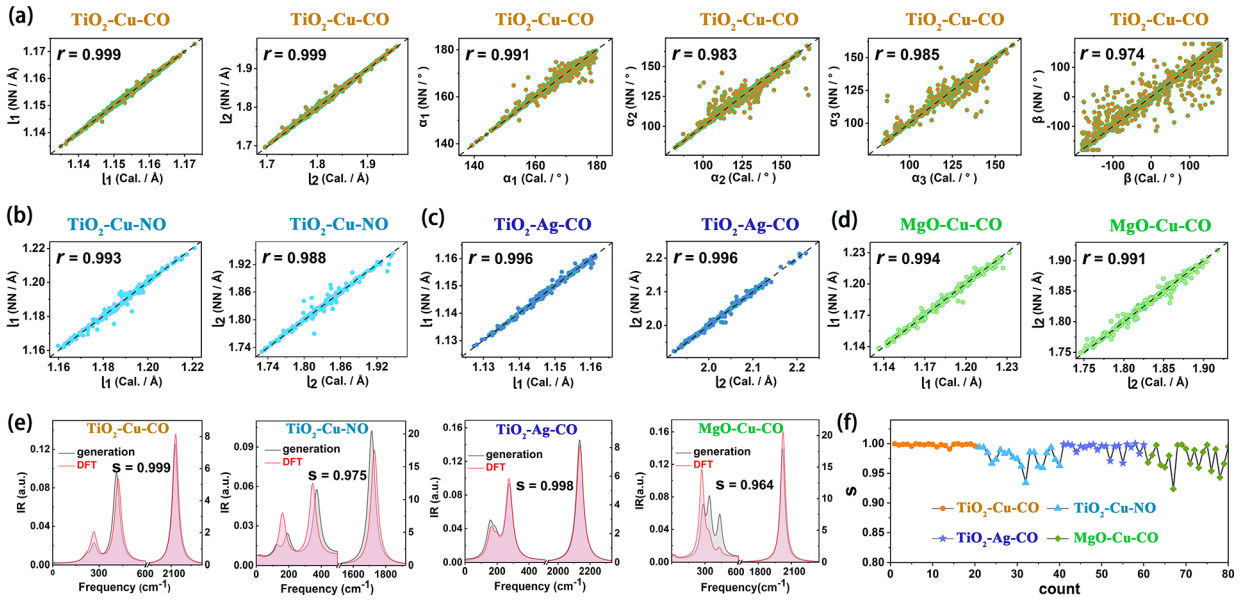

Figure 3. Predicted results of the ML-2 model for the adsorbed molecular structure information and verified the correctness of the ML-2 model by comparing the randomly generated spectra and the DFT-calculated spectra. (a) Predicted the CO information on the TiO_2−Cu−CO system including two bond lengths, three bond angles, and one dihedral angle. (b−d) Predicted the adsorbed molecular two bond lengths of the TiO_2−Cu−NO, TiO_2−Ag−CO, and MgO−Cu−CO transfer systems, respectively. (e) Verified the correctness of the ML-2 model using the Spearman correlation coefficient for the TiO_2−Cu−CO system and other TiO_2−Cu−NO, TiO_2−Ag−CO, and MgO−Cu−CO transfer systems. (f) Calculated Spearman correlation coefficient between 20 randomly generated spectra and corresponding DFT-calculated spectra for the TiO_2−Cu−CO system and other TiO_2−Cu−NO, TiO_2−Ag−CO, and MgO−Cu−CO transfer systems.

the vibrational frequencies (freq1−freq6) and IR intensities (ir1−ir6), which were selected as spectroscopic descriptors.

To begin, we conducted a correlation analysis for the vibrational spectral descriptors (Figure S2). The high-frequency signals (modes 5−6) exhibit stronger importance, especially for the C−O and C−Cu bond lengths. It is not difficult to understand since the change of bond lengths necessarily affects the frequency of the stretching vibration. However, low-frequency signals (modes 1−4) also play an indispensable role in predicting properties, angles, and dihedral. Thus, building efficient ML models is necessary for exploring the quantitative spectra structure−property relationship.

The first neural network (ML-1), a multitasking network that can spare computational resources and boost the model's generalization and transferability, was employed to predict the intricate nonlinear relationships between the spectrum and properties (Figure 2a). The key metric of an ML model is its applicability to other systems. Therefore, we examined the transferability of the above well-trained NN models for predicting properties in different catalytic systems. For the transfer systems, about 1200 adsorption configurations were extracted from the MD simulation trajectories. The ML-1 model was first transferred to the systems with new diatomic molecules such as NO, O_2, and N_2. Through transfer learning, all of them exhibited excitingly good correlations between the predicted and calculated values (Figures 2b and S3), suggesting a wide range of gas applicability. Then, the ML-1 model was transferred to the systems with new metal elements such as Ag, Fe, and Co. A slight decrease in prediction performance for a few target values was observed; however, the models are still acceptable with all correlations above 0.91 (Figures 2c and S4). Furthermore, the ML-1 model was transferred to the system with a new metal oxide carrier such as MgO, which is a very challenging task because of the large change in the structure. Surprisingly, the transferred models predicted very well (Figure 2d). We believe that the success of the transfer learning can be attributed to the use of a spectroscopic descriptor. For significant changes such as the metal oxide carrier, conventional descriptors such as the structure cannot be unified in data dimensions, and model transfer is even more impossible. The spectroscopic descriptor is able to pack the microenvironment information on the catalytic activity center into the same format and the same dimension, so the models based on it have a broader scope of application.

Besides the prediction of properties by ML-1, another multitask neural network ML-2 was also developed to establish the spectroscopy−structure relationship. Six structural parameters including two bond lengths, three bond angles, and one dihedral angle for diatomic molecules were predicted by spectroscopic descriptor (Figure 3a). The wide transferability of ML-2 was also examined in other systems, and all exhibited a high prediction accuracy (Figures 3b−d and S5−S11). The success of ML-2 allows us for the first time to accurately locate the spatial coordinates of molecule based on its vibrational spectral signals, which is the desired structural inversion. To determine the accuracy of such inversion, a validation process was designed: we randomly generated a brand-new spectrum that was not in the previous data set. Then, it was used to inverse the positions of the adsorbed molecules. The predicted structure was again taken for the first-principles calculation of the spectrum. Finally, the calculated spectrum was compared with the randomly generated spectrum at the beginning. We performed the above-mentioned process in both the initial catalytic system (TiO_2−Cu−CO) and different types of transferred systems (different diatomic molecules, transition metals, and metal oxides). As shown in Figures 3e and S12, all

https://doi.org/10.1021/jacs.3c09299
J. Am. Chem. Soc. 2023, 145, 26817−26823

of them exhibit excitingly good correlations between the randomly generated spectra and theoretically inversed spectra. The peak frequencies of the vibrational spectra and the intensities in the high-frequency region are usually well matched, while the intensities in the low-frequency region have minor differences in the transferred catalytic systems. This is an expected result, on the one hand, because the accuracy of the transferred ML models is slightly lower. On the other hand, because the IR intensity of the low-frequency region is very low, a subtle absolute error will show a large relative difference. The structures from the spectral inversion are shown in Figures S13 and S14, inspiring us to believe that the spectra may be able to help us achieve catalytic structure design by AI generation, which will be discussed in detail later. Here, we totally generated 20 random spectra in each catalytic system and conducted the structure inversion and spectra comparison. Most of the samples have a correlation greater than 0.85 between the generated and calculated spectra (Figures 3f and S15). This validation task indicates that although spectra are low-dimensional data compared with structure, it is feasible to inverse parts of key structural information from spectra. Just as what we did, only the spatial relative coordinates of diatomic molecules in the catalytic systems were inverted, and the whole structure of the catalyst remained unchanged.

An optimal catalytic activity is usually achieved when the adsorption energy falls within a not-strong-not-weak range. Thus, control of the adsorption state of the molecule is desired. One of the challenges is to determine in real time whether the molecule has reached the appropriate adsorption position. The above successful structure inversion from spectra provides a proof-of-concept catalytic structure design protocol. Because the ML-1 model can give the adsorption energy from the spectrum instantly, we can find the spectra corresponding to the desired adsorption energy by continuously generating spectra. Then, the structure inversion from the spectra was performed by ML-2, and the adsorption energies of these inversed structures were verified via DFT calculations. It should be noted that one adsorption energy can correspond to a number of different structures/spectra; thus, we collected 50 spectra for each desired adsorption energy. We first examined the TiO_2−Cu−CO system and set a series of continuous target adsorption energies (from −2.1 to −1.4 eV with an interval of 0.1 eV). All of them achieved satisfactory results, which showed that the average adsorption energy of most samples was in good agreement with the target adsorption energy (Figure 4a). Then, in different types of transferred systems, similar results were obtained during the same examination (Figures 4b−d and S16). These results indicate the feasibility of continuous catalytic structure design by AI generating with a spectroscopic descriptor.

CONCLUSIONS

To summarize, a quantitative spectra structure−property relationship was established by ML with a spectroscopic descriptor. The neural network models can predict the catalytic properties such as adsorption energy and charge transfer and invert structural parameters. To the best of our knowledge, this is the first time that the entire structure of the adsorbed molecule can be completely inverted in adsorbate−substrate catalytic systems. This is a qualitative breakthrough that makes it possible to track the catalytic reactions of molecules by spectroscopy. Moreover, it also allows the catalytic structure

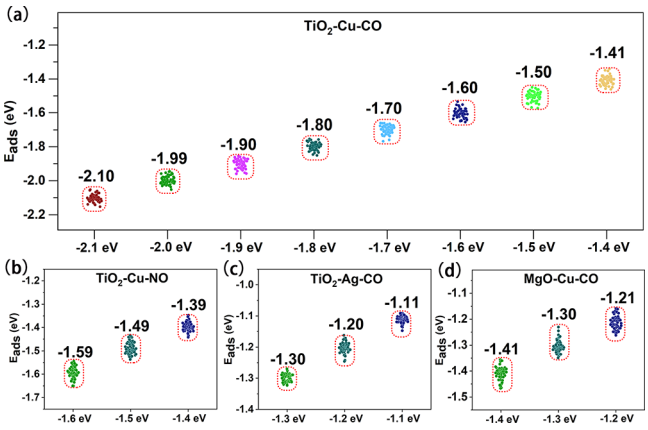

Figure 4. Screened 50 spectra based on desired adsorption energy and inverse catalytic structures using the ML-2 model for DFT validation. (a)−(d) TiO_2−Cu−CO, TiO_2−Cu−NO, TiO_2−Ag−CO, and MgO−Cu−CO systems, respectively. The horizontal axis indicates the desired adsorption energy, and the vertical axis indicates the adsorption energy by DFT. The average adsorption energy is shown on the graph.

design by AI to generate a measurable physical quantity, namely, the spectroscopic descriptor. In this work, we provide practical and detailed processes to perform structural inversion and catalytic customization through several validation tasks. Due to the universality of spectroscopic descriptors, these ML models and processes can be widely transferred to other systems including different adsorbates, metal single-atom sites, and substrates. Thus, we believe that they can also be transferred to process the in situ and real-time experimental spectral data. More generally, the inversion of high-dimensional structures from low-dimensional spectra is usually considered an impossible task, but our work showcases that the spectroscopic descriptor contains global information and artificial intelligence can establish complex cross-dimensional corresponding relationships.

METHODS

Ab Initio Molecular Dynamic Simulation. Ab initio molecular dynamic (AIMD) simulation with the hybrid Gaussian plane wave (GPW)[30] scheme was implemented in CP2K package to study the TiO_2−Cu−CO hybrid system and other transfer systems (TiO_2−Cu−NO, TiO_2−Cu−N_2, TiO_2−Cu−O_2, TiO_2−Fe−CO, TiO_2−Co−CO, TiO_2−Ag−CO, and MgO−Cu−CO). We employed the quickstep method with a plane wave cutoff of 500 Ry and the Goedecker-Teter-Hutter pseudopotentials to describe the rest of the core electrons. We also used the Perdew−Burke−Ernzerhof (PBE) exchange-correlation functional[31] and the Grimme-D3 dispersion correction[32] to account for the exchange-correlation effects and the van der Waals interactions, respectively. The localized double ξ-valence-polarized (DZVP) basis set[33] was used to expand the wave functions in all calculations. In our study of the TiO_2−Cu−CO hybrid system, we employed AIMD simulations in the canonical ensemble (NVT) to gain insight into its behavior. The simulation was run for a duration of 5 ps, while other transfer systems were run for 1.4 ps with a step size of 0.5 fs. After allowing the system to equilibrate for 1 ps, we collected configurations at regular intervals of two steps to analyze the results. To explore the configure space more comprehensively, all systems for 5 ps were run at three different temperatures (200, 300, and 400 K), using a Nose-Hoover thermostat.[34] The charge transfer of CO was calculated by using the Bader charge method.

Static Calculation. We performed static calculations for all configurations by Vienna ab initio simulation package with a plane-wave energy cutoff of 400 eV. We described the exchange-correlation

https://doi.org/10.1021/jacs.3c09299
J. Am. Chem. Soc. 2023, 145, 26817−26823

energy by the generalized gradient approximation (GGA) with PBE functional. The projector augmented wave method[35] was used for the ion-electron interaction. Long-range van der Waals (vdW) interactions were corrected by Grimme's DFT-D3 method. The surface Brillouin zone was sampled with 3 × 3 × 1 Monkhorst−Pack k-mesh, and the vacuum space was set to ∼15 Å. All the structures were completed until the energies converged to 10^{-5} eV. We investigated the charge transfer between CO molecules and the substrate by using the Bader charge analysis method.

The adsorption energies of E_{ads} were calculated as follows:

$$E_{ads} = E_{sub@mol} - E_{sub} - E_{mol}$$

where $E_{sub@mol}$ represents the total energy of the small molecule adsorbed on the metal oxide substrate, E_{sub} is the energy of the metal oxide, and E_{mol} is the energy of small molecule.

IR Spectral Calculation. The adsorption state of small molecules was mainly affected by the metal oxide surface, so we applied the cluster model cut from the first layer of the periodic model system for spectral calculation. The infrared spectra were computed by Gaussian 16 package[36] with the PBE functional and 6-31 + G** basis sets for major elements and pseudo LANL2DZ basis sets[37] for metal atoms.

Neural Network Architecture. We used a neural network (NN) with one input layer, five hidden layers, and one output layer to predict the adsorption state of the TiO_2−Cu−CO hybrid system based on infrared spectra as descriptors. The adsorption state included adsorption energy, charge transfer, and structural information (bond length, bond angle, and dihedral). Each hidden layer consisted of 1024 neurons, and 80% of the data set was used for training and 20% of the data set was selected for validation. We used the rectified linear unit (ReLU) as the activation function[38] to establish the correlation between the descriptors and prediction targets. The mean absolute error (MAE) was applied as the loss function to measure the average magnitude of the error between the predicted and true values. To optimize the model parameters, the adaptive moment estimation (Adam) algorithm and the learning rate decay strategy were implemented in TensorFlow.[39] We used a maximum learning rate of 0.001 and a batch size of 120, which allowed us to update the model parameters after 120 samples in each iteration. The model with the last four hidden layers frozen was used to train for transfer systems and then to fine-tune it with a maximum learning rate of 0.0001 after unfreezing all layers. We used a batch size of 12 and a dropout rate of 0.1 for other transfer learning systems to reduce overfitting in neural networks by randomly dropping out some neurons during training.

■ ASSOCIATED CONTENT

Supporting Information

The Supporting Information is available free of charge at https://pubs.acs.org/doi/10.1021/jacs.3c09299.

CO structure information; importance of the spectroscopy descriptors; ML-1 model for catalytic properties; ML-2 model for the NO structure information; ML-2 model for the CO structure information; ML-2 model for the N_2 structure information; ML-2 model for the O_2 structure information; correctness of the ML-2 model; electronic structures inversed on the basis of the randomly generated spectra; calculated Spearman's correlation coefficient; and 50 spectra based on desired adsorption energy (PDF)

■ AUTHOR INFORMATION

Corresponding Authors

Yan Huang − *Key Laboratory of Precision and Intelligent Chemistry, School of Chemistry and Materials Science, University of Science and Technology of China, Hefei, Anhui 230026, China*; Email: hyan@ustc.edu.cn

Song Wang − *Key Laboratory of Precision and Intelligent Chemistry, School of Chemistry and Materials Science, University of Science and Technology of China, Hefei, Anhui 230026, China*; orcid.org/0000-0003-1252-8091; Email: wsong09@ustc.edu.cn

Jun Jiang − *Key Laboratory of Precision and Intelligent Chemistry, School of Chemistry and Materials Science, University of Science and Technology of China, Hefei, Anhui 230026, China*; orcid.org/0000-0002-6116-5605; Email: jiangj1@ustc.edu.cn

Authors

Tongtong Yang − *Key Laboratory of Precision and Intelligent Chemistry, School of Chemistry and Materials Science, University of Science and Technology of China, Hefei, Anhui 230026, China; Institute of Intelligent Innovation, Henan Academy of Sciences, Zhengzhou, Henan 451162, P. R. China*

Donglai Zhou − *Key Laboratory of Precision and Intelligent Chemistry, School of Chemistry and Materials Science, University of Science and Technology of China, Hefei, Anhui 230026, China*

Sheng Ye − *School of Artificial Intelligence, Anhui University, Hefei, Anhui 230601, China*

Xiyu Li − *Songshan Lake Materials Laboratory, Dongguan, Guangdong 523808, China*

Huirong Li − *Key Laboratory of Precision and Intelligent Chemistry, School of Chemistry and Materials Science, University of Science and Technology of China, Hefei, Anhui 230026, China*

Yi Feng − *Key Laboratory of Precision and Intelligent Chemistry, School of Chemistry and Materials Science, University of Science and Technology of China, Hefei, Anhui 230026, China*

Zifan Jiang − *Key Laboratory of Precision and Intelligent Chemistry, School of Chemistry and Materials Science, University of Science and Technology of China, Hefei, Anhui 230026, China*

Li Yang − *Institutes of Physical Science and Information Technology, Anhui University, Hefei, Anhui 230601, China*

Ke Ye − *Key Laboratory of Precision and Intelligent Chemistry, School of Chemistry and Materials Science, University of Science and Technology of China, Hefei, Anhui 230026, China*

Yixi Shen − *Key Laboratory of Precision and Intelligent Chemistry, School of Chemistry and Materials Science, University of Science and Technology of China, Hefei, Anhui 230026, China*

Shuang Jiang − *Key Laboratory of Precision and Intelligent Chemistry, School of Chemistry and Materials Science, University of Science and Technology of China, Hefei, Anhui 230026, China*

Shuo Feng − *Key Laboratory of Precision and Intelligent Chemistry, School of Chemistry and Materials Science, University of Science and Technology of China, Hefei, Anhui 230026, China*; orcid.org/0000-0003-0530-8381

Guozhen Zhang − *Key Laboratory of Precision and Intelligent Chemistry, School of Chemistry and Materials Science, University of Science and Technology of China, Hefei, Anhui 230026, China*; orcid.org/0000-0003-0125-9666

Complete contact information is available at: https://pubs.acs.org/10.1021/jacs.3c09299

Author Contributions

[#]T.Y., D.Z., S.Y., and X.L. contributed equally to this work. All authors discussed the results and commented on the manuscript.

Notes

The authors declare no competing financial interest.

■ ACKNOWLEDGMENTS

This work was financially supported by the Innovation Program for Quantum Science and Technology (2021ZD0303303), the CAS Project for Young Scientists in Basic Research (YSBR-005), the National Natural Science Foundation of China (Grant No. 22025304, 22033007, 22203082, 12227901, and 22203001), the University Synergy Innovation Program of Anhui Province (GXXT-2022-062), the Natural Science Foundation of Anhui Province (Grants 2208085Y04) and the Fundamental Research Funds for the Central Universities. We thank the Hefei Advanced Computing Center for providing numerical computations and the USTC supercomputing center for providing computational resources for this project.

■ REFERENCES

(1) Datye, A. K.; Votsmeier, M. Opportunities and challenges in the development of advanced materials for emission control catalysts. *Nat. Mater.* **2021**, *20*, 1049−1059.
(2) Jin, Z.; Wang, L.; Zuidema, E.; Mondal, K.; Zhang, M.; Zhang, J.; Wang, C.; Meng, X.; Yang, H.; Mesters, C.; Xiao, F.-S. Hydrophobic zeolite modification for in situ peroxide formation in methane oxidation to methanol. *Science* **2020**, *367*, 193−197.
(3) Yang, T.; Mao, X.; Zhang, Y.; Wu, X.; Wang, L.; Chu, M.; Pao, C.-W.; Yang, S.; Xu, Y.; Huang, X. Coordination tailoring of Cu single sites on C_3N_4 realizes selective CO_2 hydrogenation at low temperature. *Nat. Commun.* **2021**, *12*, 6022.
(4) Men, Y.; Su, X.; Li, P.; Tan, Y.; Ge, C.; Jia, S.; Li, L.; Wang, J.; Cheng, G.; Zhuang, L.; Chen, S.; Luo, W. Oxygen-inserted top-surface layers of Ni for boosting alkaline hydrogen oxidation electrocatalysis. *J. Am. Chem. Soc.* **2022**, *144*, 12661−12672.
(5) Griffiths, J.; Földes, T.; de Nijs, B.; Chikkaraddy, R.; Wright, D.; Deacon, W. M.; Berta, D.; Readman, C.; Grys, D. B.; Rosta, E.; Baumberg, J. J. Resolving sub-angstrom ambient motion through reconstruction from vibrational spectra. *Nat. Commun.* **2021**, *12*, 6759.
(6) Dan, Y.; Zhao, Y.; Li, X.; Li, S.; Hu, M.; Hu, J. Generative adversarial networks (GAN) based efficient sampling of chemical composition space for inverse design of inorganic materials. *npj Comput. Mater.* **2020**, *6*, 84.
(7) Jin, Z.; Li, P.; Meng, Y.; Fang, Z.; Xiao, D.; Yu, G. Understanding the inter-site distance effect in single-atom catalysts for oxygen electroreduction. *Nat. Catal.* **2021**, *4*, 615−622.
(8) Li, X.; Wang, S.; Li, L.; Sun, Y.; Xie, Y. Progress and perspective for in situ studies of CO_2 reduction. *J. Am. Chem. Soc.* **2020**, *142*, 9567−9581.
(9) Bai, X.; Zhao, X.; Zhang, Y.; Ling, C.; Zhou, Y.; Wang, J.; Liu, Y. Dynamic stability of copper single-atom catalysts under working conditions. *J. Am. Chem. Soc.* **2022**, *144*, 17140−17148.
(10) Sarma, B. B.; Plessow, P. N.; Agostini, G.; Concepción, P.; Pfänder, N.; Kang, L.; Wang, F. R.; Studt, F.; Prieto, G. Metal-specific reactivity in single-atom catalysts: CO oxidation on 4d and 5d transition metals atomically dispersed on MgO. *J. Am. Chem. Soc.* **2020**, *142*, 14890−14902.
(11) Tang, Y.; Asokan, C.; Xu, M.; Graham, G. W.; Pan, X.; Christopher, P.; Li, J.; Sautet, P. Rh single atoms on TiO_2 dynamically respond to reaction conditions by adapting their site. *Nat. Commun.* **2019**, *10*, 4488.
(12) Jeon, H. S.; Timoshenko, J.; Rettenmaier, C.; Herzog, A.; Yoon, A.; Chee, S. W.; Oener, S.; Hejral, U.; Haase, F. T.; Roldan Cuenya, B. Selectivity control of Cu nanocrystals in a gas-fed flow cell through CO_2 pulsed electroreduction. *J. Am. Chem. Soc.* **2021**, *143*, 7578−7587.
(13) Chang, X.; Vijay, S.; Zhao, Y.; Oliveira, N. J.; Chan, K.; Xu, B. Understanding the complementarities of surface-enhanced infrared and Raman spectroscopies in CO adsorption and electrochemical reduction. *Nat. Commun.* **2022**, *13*, 2656.
(14) Shaaban, E.; Li, G. Probing active sites for carbon oxides hydrogenation on Cu/TiO_2 using infrared spectroscopy. *Commun. Chem.* **2022**, *5*, 32.
(15) Begušić, T.; Blake, G. A. Two-dimensional infrared-Raman spectroscopy as a probe of water's tetrahedrality. *Nat. Commun.* **2023**, *14*, 1950.
(16) Dodo, K.; Fujita, K.; Sodeoka, M. Raman spectroscopy for chemical biology research. *J. Am. Chem. Soc.* **2022**, *144*, 19651−19667.
(17) Conti, I.; Cerullo, G.; Nenov, A.; Garavelli, M. Ultrafast spectroscopy of photoactive molecular systems from first principles: Where we stand today and where we are going. *J. Am. Chem. Soc.* **2020**, *142*, 16117−16139.
(18) Taghizadeh, A.; Leffers, U.; Pedersen, T. G.; Thygesen, K. S. A library of ab initio Raman spectra for automated identification of 2D materials. *Nat. Commun.* **2020**, *11*, 3011.
(19) Ye, S.; Zhong, K.; Zhang, J.; Hu, W.; Hirst, J. D.; Zhang, G.; Mukamel, S.; Jiang, J. A machine learning protocol for predicting protein infrared spectra. *J. Am. Chem. Soc.* **2020**, *142*, 19071.
(20) Han, Z.-K.; Sarker, D.; Ouyang, R.; Mazheika, A.; Gao, Y.; Levchenko, S. V. Single-atom alloy catalysts designed by first-principles calculations and artificial intelligence. *Nat. Commun.* **2021**, *12*, 1833.
(21) Ren, H.; Zhang, Q.; Wang, Z.; Zhang, G.; Liu, H.; Guo, W.; Mukamel, S.; Jiang, J. Machine learning recognition of protein secondary structures based on two-dimensional spectroscopic descriptors. *Proc. Natl. Acad. Sci. U.S.A.* **2022**, *119*, No. e2202713119.
(22) Wang, X.; Jiang, S.; Hu, W.; Ye, S.; Wang, T.; Wu, F.; Yang, L.; Li, X.; Zhang, G.; Chen, X.; Jiang, J.; Luo, Y. Quantitatively determining surface-adsorbate properties from vibrational spectroscopy with interpretable machine learning. *J. Am. Chem. Soc.* **2022**, *144*, 16069−16076.
(23) Chong, Y.; Huo, Y.; Jiang, S.; Wang, X.; Zhang, B.; Liu, T.; Chen, X.; Han, T.; Smith, P. E. S.; Wang, S.; Jiang, J. Machine learning of spectra-property relationship for imperfect and small chemistry data. *Proc. Natl. Acad. Sci. U. S. A.* **2023**, *120*, No. e2220789120.
(24) Hulva, J.; Meier, M.; Bliem, R.; Jakub, Z.; Kraushofer, F.; Schmid, M.; Diebold, U.; Franchini, C.; Parkinson, G. S. Unraveling CO adsorption on model single-atom catalysts. *Science* **2021**, *371*, 375−379.
(25) Lee, B. H.; Park, S.; Kim, M.; Sinha, A. K.; Lee, S. C.; Jung, E.; Chang, W. J.; Lee, K. S.; Kim, J. H.; Cho, S. P.; Kim, H.; Nam, K. T.; Hyeon, T. Reversible and cooperative photoactivation of single-atom Cu/TiO_2 photocatalysts. *Nat. Mater.* **2019**, *18*, 620−626.
(26) Shangguan, W.; Liu, Q.; Wang, Y.; Sun, N.; Liu, Y.; Zhao, R.; Li, Y.; Wang, C.; Zhao, J. Molecular-level insight into photocatalytic CO_2 reduction with H_2O over Au nanoparticles by interband transitions. *Nat. Commun.* **2022**, *13*, 3894.
(27) Zhang, X.; Li, J.; Li, Y.-Y.; Jung, Y.; Kuang, Y.; Zhu, G.; Liang, Y.; Dai, H. Selective and high current CO_2 electro-reduction to multicarbon products in near-neutral KCl electrolytes. *J. Am. Chem. Soc.* **2021**, *143*, 3245−3255.
(28) Tcharkhetian, A. E. G.; Bruni, A. T.; Rodrigues, C. H. P. Combining experimental and theoretical approaches to study the structural and spectroscopic properties of Flakka (α-pyrrolidinopentiophenone). *Res. Chem.* **2021**, *3*, No. 100254.
(29) Böselt, L.; Aerts, R.; Herrebout, W.; Riniker, S. Improving the IR spectra alignment algorithm with spectra deconvolution and

https://doi.org/10.1021/jacs.3c09299
J. Am. Chem. Soc. 2023, 145, 26817−26823

combination with Raman or VCD spectroscopy. *Phys. Chem. Chem. Phys.* **2023**, *25*, 2063−2074.
(30) VandeVondele, J.; Krack, M.; Mohamed, F.; Parrinello, M.; Chassaing, T.; Hutter, J. Quickstep: Fast and accurate density functional calculations using a mixed Gaussian and plane waves approach. *Comput. Phys. Commun.* **2005**, *167*, 103−128.
(31) Perdew, J. P.; Burke, K.; Ernzerhof, M. Generalized gradient approximation made simple. *Phys. Rev. Lett.* **1996**, *77*, 3865−3868.
(32) Grimme, S.; Antony, J.; Ehrlich, S.; Krieg, H. A consistent and accurate ab initio parametrization of density functional dispersion correction (DFT-D) for the 94 elements H-Pu. *J. Chem. Phys.* **2010**, *132*, 154104.
(33) VandeVondele, J.; Hutter, J. Gaussian basis sets for accurate calculations on molecular systems in gas and condensed phases. *J. Chem. Phys.* **2007**, *127*, 114105.
(34) Nosé, S. Constant temperature molecular dynamics methods. *Prog. Theor. Phys. Suppl.* **1991**, *103*, 1−46.
(35) Blöchl, P. E. Projector augmented-wave method. *Phys. Rev. B: Condens. Matter Mater. Phys.* **1994**, *50*, 17953−17979.
(36) Yang, D.; Hu, X.; Xie, D. Quantum dynamics of vibration-vibration energy transfer for vibrationally excited HF colliding with H_2. *J. Comput. Chem.* **2019**, *40*, 1084−1090.
(37) Hay, P. J.; Wadt, W. R. Ab initio effective core potentials for molecular calculations. Potentials for K to Au including the outermost core orbitals. *J. Chem. Phys.* **1985**, *82*, 299−310.
(38) Maas, A. L.; Hannun, A. Y.; Ng, A. Y. Rectifier nonlinearities improve neural network acoustic models. *Proc. ICML* **2013**, *30*, 3.
(39) Abadi, M.; Barham, P.; Chen, J.; Chen, Z.; Davis, A.; Dean, J.; Devin, M.; Ghemawat, S.; Irving, G.; Isard, M.; Kudlur, M.; Levenberg, J.; Monga, R.; Moore, S.; Murray, D. G.; Steiner, B.; Tucker, P.; Vasudevan, V.; Warden, P.; Wicke, M.; Yu, Y.; Zheng, X. Tensorflow: a system for large-scale machine learning. *Proceedings of the 12th USENIX Symposium on Operating Systems Design and Implementation (OSDI'16)*, 2016; pp. 265−283.

https://doi.org/10.1021/jacs.3c09299
J. Am. Chem. Soc. 2023, 145, 26817−26823